Appl Phys B (2008) 93: 515–520
DOI 10.1007/s00340-008-3210-4

**Applied Physics B**
**Lasers and Optics**

# All-semiconductor laser driven terahertz time-domain spectrometer

**C. Jördens · T. Schlauch · M. Li · M.R. Hofmann · M. Bieler · M. Koch**

Received: 27 June 2008 / Revised version: 18 August 2008 / Published online: 17 September 2008
© Springer-Verlag 2008

**Abstract** We present a terahertz time-domain spectrometer pumped by an all-semiconductor femtosecond laser system which emits 600 fs long optical pulses at 830 nm. Standard LT-GaAs antennas are used to generate and coherently detect THz radiation with a bandwidth of 1.4 THz. The measured time traces are in good agreement with simulations based on the Drude–Lorentz model. Spectroscopic measurements on polymers with different additive contents as well as THz imaging were carried out to confirm the successful operation of the spectrometer. Our approach holds great potential for the development of cost-effective, rugged and portable THz spectrometers for a variety of applications.

**PACS** 42.55.Px · 42.65.Re · 07.57.Hm · 07.57.Kp · 42.62.Cf

## 1 Introduction

In the last decade the use of terahertz (THz) spectroscopy systems greatly increased. At the beginning standard spectroscopy was the most prominent task. Recently, the range of applications has become much broader. Such systems can be employed for the detection of drugs and explosives in the field of homeland security [1, 2]. Furthermore, non-destructive testing (NDT), which has been so far dominated by X-ray, ultrasound and thermograph measurements, benefits as well from this young technology. A wide range of suitable NDT applications has already been shown. The detection of defects in SOFI foam [3] or the determination of the additive content in plastic compounds [4] both are just two out of many examples. Pulsed THz radiation can be used to investigate the fiber orientation in plastics [5] as well as to detect foreign bodies in food [6]. Furthermore, the measurement of the humidity content in pharmaceuticals [7] and the leave water content in plants [8, 9], both of which can be performed non-contactless and non-invasive, illustrate the importance of THz spectroscopy. Recently, even the detection of hidden paintings was demonstrated by Fukunaga et al. [10, 11].

The generation and coherent detection of THz radiation is usually accomplished via an optoelectronic approach based on photoconductive antennas, which are illuminated with laser radiation. The radiation can be either continuous (cw) [12, 13] or pulsed [14]. The use of either technique has its own advantages and disadvantages. Pulsed THz spectroscopy is a powerful tool which provides much information on the sample. It is used for most applications of non-destructive testing mentioned in the first paragraph. The amplitude and phase of the measured THz traces can be taken to derive the complex refractive index of a material [15]. Unfortunately, pulsed systems usually require a bulky and expensive femtosecond Ti:sapphire laser. Continuous wave systems based on photomixing are more cost-effective due to the use of semiconductor lasers. To obtain the same information as with a pulsed system time-consuming frequency scans are required. The use of semiconductor lasers could also make THz time-domain systems

C. Jördens (✉) · M. Koch
Institut für Hochfrequenztechnik, TU Braunschweig, Schleinitzstr. 22, 38106 Braunschweig, Germany
e-mail: ch.joerdens@tu-bs.de

T. Schlauch · M. Li · M.R. Hofmann
Lehrstuhl für Photonik und THz-Technologie, Ruhr-Universität Bochum, Universitätsstrasse 150, 44780 Bochum, Germany

M. Bieler
Physikalisch-Technische Bundesanstalt, Bundesallee 100, 38116 Braunschweig, Germany

cost-effective. Yet, laser pulses emitted from semiconductor lasers are typically much longer [16–19] than those supplied by Ti:sapphire lasers. Due to the longer laser pulse duration one can expect a smaller THz signal amplitude and a reduced THz bandwidth. Nevertheless, a smaller bandwidth is sufficient for many NDT applications, since the absorption increases strongly with increasing frequency for most materials, anyway. Altogether, the drawback of a reduced bandwidth of a semiconductor laser based system can be overcompensated for by its reduced price.

As an alternative, femtosecond fiber lasers have already been used to generate THz radiation [20–23]. Such laser systems are more stable than Ti:sapphire lasers, but they are still relatively expensive. However, due to the longer emission wavelength of fiber lasers (1550 nm) one inevitably relies on different antenna substrates, e.g., LT-InGaAs, for the THz emission and detection. Those substrates are more difficult to fabricate, and are still under development. Furthermore, they are, according to our experience [23], very fragile, since they are much more sensitive to electromagnetic discharge compared with LT-GaAs. For NDT applications the main emphasis lies on stability and robustness of the system including the antennas.

Besides lasers at 1550 nm there are also Yb-doped ultrashort-pulse fiber laser at 1045 nm available. Recently, such a laser has been used to generate and detect THz radiation with a CdTe crystal [24]. If a photoconductive antenna is used for the detection the choice of the semiconductor substrate strongly affects the achievable bandwidth and signal-to-noise ratio. GaBiAs shows much better detector performance at wavelengths around 1 μm than InGaAs [25].

In this paper, we present a THz time-domain spectrometer with coherent detection driven by an all-semiconductor femtosecond laser system emitting optical pulses at 830 nm. The laser system consists of a laser diode, a tapered amplifier, and an external pulse compressor altogether mounted on a breadboard forming a stable and transportable unit. Besides its robustness the laser system offers an impressive peak power of 2.5 kW. With the THz system we achieve a bandwidth of 1.4 THz. Our approach combines cost-effective semiconductor lasers with highly developed LT-GaAs antennas and, thus, provides the basis for future economic, broadband, and sensitive THz spectrometers.

## 2 Femtosecond semiconductor laser system

Here, we employ a laser system which generates high peak power femtosecond pulses from an amplified passively mode-locked diode laser [17, 18] with external pulse compression. So far, ultrashort semiconductor lasers have longer pulse durations and lower output powers compared with ultrashort Ti:sapphire lasers. We use an external pulse compression unit [26, 27] to compensate for the extensive chirp

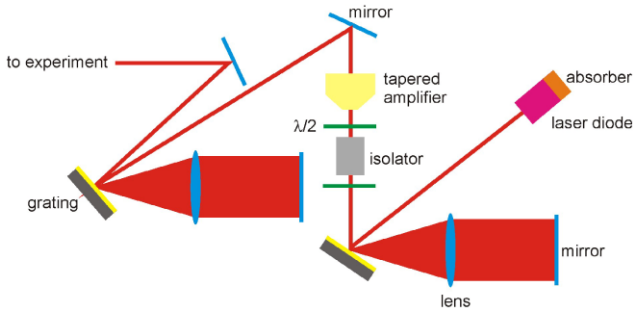


**Fig. 1** Experimental setup with oscillator (*right-hand side*), compressor (*left-hand side*) and tapered amplifier. λ/2-plates ensure required polarization

of the active semiconductor region and to achieve a sub-picosecond pulse width. Moreover, we obtain a high peak power by external amplification of the laser pulses [19, 28].

The laser system (see Fig. 1) consists of a laser diode in an external cavity, a tapered amplifier, and a compact external pulse compressor. The laser diode consists of a gain section (1200 μm) and an absorber section with a length of 80 μm. The latter one is operated at reverse bias and acts as saturable absorber [16]. The first-order diffraction of the grating is guided to the Fourier lens ($f = 100$ mm) that focuses the spectral components onto the end mirror. The laser emission is coupled out of the cavity by the 0th order reflection from the grating.

The laser radiation is focused into the front faced of the tapered amplifier. It consists of an index-guided ridge waveguide section and gain-guided tapered section both with a length of 2000 μm, respectively. The index-guiding allows for the propagation of only one single mode. The beam profile at the output of the amplifier is corrected by an aspherical lens ($f = 6.24$ mm) and a cylindrical lens ($f = 50$ mm). Thereafter, the radiation is guided into an external pulse compressor which has a similar design as the external cavity of the oscillator. It consists of a grating, a lens ($f = 150$ mm), and a high reflection end mirror. The linear and the square chirp of the optical pulses can be compensated by shifting and rotating the lens, respectively.

We measured several amplified and compressed pulses which showed all pulse durations around 600 fs. The autocorrelation trace and the spectrum of one selected measurement are depicted in Fig. 2. A pulse width of 622 fs at a spectral width of 1.83 THz is achieved. The pulse shape is best fit by a Lorentzian. For the time-bandwidth product we calculate a value of 1.138, which is still above the Fourier limit. This suggests that there might be potential for even further compression with more complex and sophisticated compressors. The emission wavelength is centered around 830 nm. With an average optical output power of 513 mW for the entire laser system and a repetition rate of 330 MHz, we obtain a peak power of 2.5 kW.

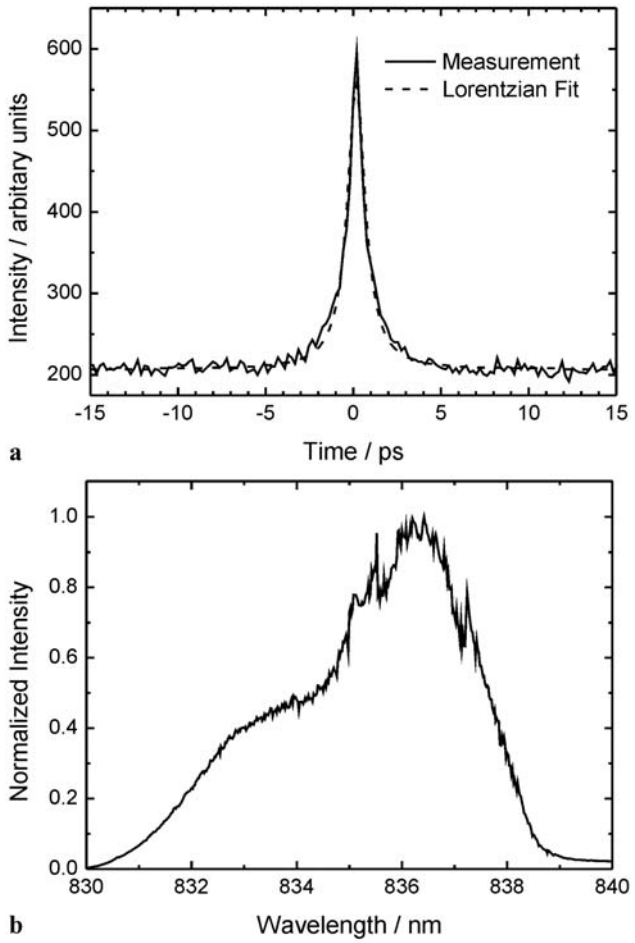


**Fig. 2** Autocorrelation trace (*solid*) with Lorentzian fit function (*dashed*) (**a**) and measured spectrum (**b**) of the compressed and amplified pulse at the output of the femtosecond laser system

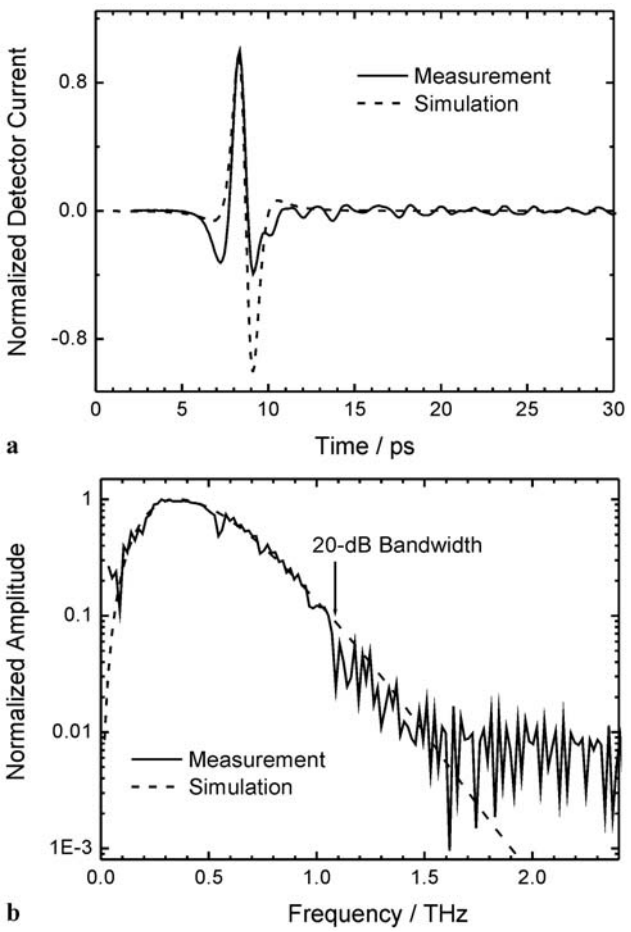


**Fig. 3** (**a**) Measured (*solid line*) and calculated (*dashed line*) terahertz pulses. (**b**) Corresponding frequency spectra

## 3 THz spectrometer and results

The semiconductor laser pulses are used to operate a standard THz time-domain transmission spectrometer [14]. The short optical pulses with an average optical power of 25 mW are focused onto the gap of the photoconductive antennas. The emitter antenna is biased with 30 V and consists of a coplanar stripline with a gap of 10 µm; the receiver is a 20 µm dipole with a 5 µm gap. Metal structures were deposited onto a standard LT-GaAs substrate. Four off-axis parabolic mirrors are used to collect the emitted THz radiation, focus it down, collect it again, and, finally, focus it onto the detector antenna. In order to obtain THz images, the sample is placed in the focus of the THz radiation. It is moved by a two-dimensional translation stage perpendicular to the THz beam. At every spatial position a THz pulse is recorded and analyzed [29, 30].

Figure 3 shows the measured THz time trace and the corresponding spectral amplitude after performing a fast Fourier transform. We achieve a bandwidth of 1.4 THz. This frequency range is ideally suited for most NDT applications mentioned in the introduction. At higher frequencies the absorption of most materials strongly increases and, hence, they are only barely transparent for frequencies above 2 THz. Consequently, many NDT applications will rely on frequencies below 1.5 THz, anyway. Examples include NDT of ceramics, polar polymers, polymeric compounds, chocolate, and plants, to name only a few.

## 4 Experimental results

To demonstrate the capability of our THz spectrometer we present the results of some first measurements in Fig. 4. We investigated the THz properties of plastics with different additive contents and took a first image. Figure 4(a) depicts the refractive index of pure polypropylene and of polypropylene filled with 40 wt% of $CaCO_3$. The refractive index was extracted from the measured THz traces. It is 1.75 and 1.52 for polypropylene with and without $CaCO_3$, respectively. These results agree well with our findings presented in [4]. The

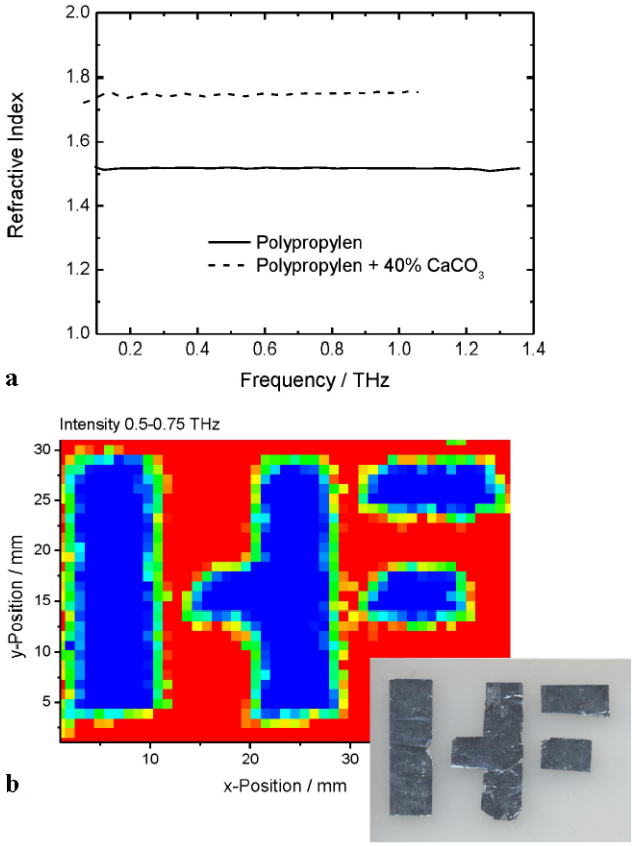


**Fig. 4** (**a**) Refractive index of polypropylen w/o $CaCO_3$. (**b**) THz transmission image of a metal structure with the capital letters IHF (see *inset*)

imaging measurement shown in Fig. 4(b) was performed on a sample which consists of the metal logo of our institute (IHF) on a 5 mm thick polyethylene substrate. A photo of the logo is shown in the inset. The THz image depicts the transmitted intensity between 0.5 and 0.75 THz on a linear scale. The metal structure of the logo is clearly reproduced in the image, see inset of Fig. 4(b). These results confirm the successful operation of a THz spectrometer driven by a femtosecond diode laser system.

## 5 Theoretical evaluation of the pulse length

The length of the optical gating pulse strongly affects the achievable THz bandwidth as discussed in [31]. For a long time pulsed semiconductor lasers have been thought not to be suited for the generation of pulsed THz radiation due to longer laser pulse durations around 1 ps. In order to determine the maximum acceptable optical pulse duration, which provides sufficient THz bandwidth for industrial applications, we additionally modeled the THz generation, propagation, and detection processes for our particular experimental situation. This allows for an estimation, of the THz bandwidth which be achieved with optical pulses of different durations.

Our calculations are based on an enhanced Drude–Lorentz model [32, 33]. The formalism was originally developed by Jepsen et al. [32], but we improve their model in two different aspects. First, to incorporate dynamical screening of the bias field we calculate the partial currents that are associated with the carriers optically generated in a given time-slot. For each time step, these currents are summed up and the accelerating electric field is recalculated. Secondly, we use partial currents also when modeling the detector response.

The current $J_{\mathrm{gen}}(t)$ which occurs in the photoconductive gap of the emitter antenna is calculated by solving a set of differential equations (see [32] for details) for the free-carrier density, the carrier velocity, and the screening field. In this calculation, we only consider electrons due to their small effective mass as compared to the hole mass. Moreover, the laser excitation pulse is not just described as a superposition of $\delta$-pulses as in [32], but interaction between carriers generated at different times is taken into account. For this calculation we assumed a carrier scattering time, trapping time, and recombination time of 30 fs, 500 fs, and 10 ps, respectively. The geometrical screening factor is 900 as proposed by Jepsen et al. [32]. The bias field applied to the laser excitation region was 30 kV/cm, as already mentioned above, and the generated carrier density was $4 \times 10^{18}$ cm$^{-3}$.

We then use linear response theory to calculate the electric THz field at the detector antenna, $E_{\mathrm{det}}(\omega) = H_{\mathrm{det}}(\omega) \cdot H_{\text{det-sub}}(\omega) \cdot H_{\mathrm{opt}}(\omega) \cdot H_{\text{em-sub}}(\omega) \cdot E_{\mathrm{gen}}(\omega)$, with $E_{\mathrm{gen}}(t) \propto \mathrm{d}J_{\mathrm{gen}}(t)/\mathrm{d}t$. $H_{\text{em-sub}}$ and $H_{\text{det-sub}}$ are transfer functions accounting for the absorption and dispersion of the THz radiation in the substrates of the emitter and detector antenna, respectively. Our formalism also considers propagation of the THz pulses from the emitter antenna to the detector antenna ($H_{\mathrm{opt}}$) and the transfer function of the detector antenna ($H_{\mathrm{det}}$). Both transfer functions are taken from [32]. $H_{\mathrm{opt}}$ accounts for the frequency dependent spot size of the THz pulses at the detector antenna. $H_{\mathrm{det}}$ depends on the physical dimensions of the receiving dipole antenna which has a total length of 20 µm (including 5 µm gap); the dipole is 20 µm broad.

Finally, the current in the detector antenna $J_{\mathrm{det}}(t)$ is obtained from a convolution of $E_{\mathrm{det}}(t)$ with the optically induced conductivity $\sigma_0(t)$ : $J_{\mathrm{det}}(t) = f_{\mathrm{rep}} \cdot [E_{\mathrm{det}}(t) * \sigma_0(t)]$, with $f_{\mathrm{rep}}$ being the repetition rate of the laser system and $*$ denoting convolution. The optically induced conductivity is derived from $\sigma_0(t) = G(t) * s_0(t)$. Here $G(t)$ is the generation term which follows the envelope of the optical gating pulse, and $s_0(t)$ is an impulse function for the detector antenna derived by Grischkowsky and Katzenellenbogen [33]. The relevant time constants of the detector substrate (scattering time and trapping time) are taken to be the same as

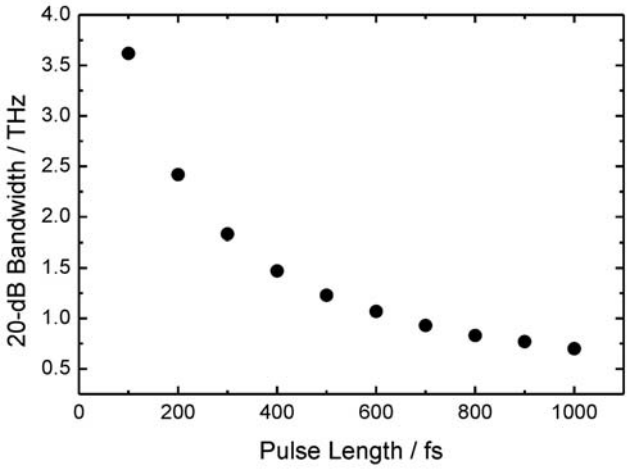


**Fig. 5** Simulated 20-dB bandwidth for optical pulses of different durations

for the emitter substrate. As for the emitter antenna, we only considered electrons contributing to the current. Although this approach considers partial currents, it neglects screening effects in the detector antenna, which is substantiated by the alternating THz field and its rather low amplitude.

Figure 5 depicts the 20-dB bandwidth which is achievable for different durations of the optical pulse. It can be observed that with increasing pulse duration the achievable bandwidth decreases substantially. For pulse durations of more than 400 fs the bandwidth drops below 1.5 THz. This result verifies that even longer pulses around 500 fs provide sufficient THz bandwidth for many NDT applications.

Furthermore, we compare our measured signal with the results for a simulation with a pulse duration of 600 fs. We obtain an excellent agreement between the calculated and measured spectra, see Fig. 3. However, the temporal shape obtained from the calculation slightly deviates from the measured shape, see Fig. 3. While the measured pulse is unipolar, the simulated pulse nearly shows a bipolar shape. We attribute this discrepancy to a misalignment and/or imperfections of optical components. Such errors will change the optical image of the THz radiation from the emission point to the detection point. The fact that our semiconductor laser does not produce a Gaussian beam profile which we considered in our calculation might also contribute to the difference between the measurement and the calculation.

## 6 Summary and conclusion

We present a THz time-domain spectroscopy system based on an all-semiconductor femtosecond laser system. The laser delivers optical pulses with an output power exceeding 500 mW and a pulse duration of 600 fs at a wavelength of 830 nm. The laser pulses are used to drive photoconductive antennas for the generation and coherent detection of THz radiation. Our spectroscopy system has a bandwidth of 1.4 THz, which is sufficient for many NDT applications such as testing of ceramics, polar polymers, polymeric compounds, and chocolate, as well as measurements of the plant water status. We have carried out first spectroscopic measurements with our system to demonstrate its successful operation. The use of femtosecond semiconductor lasers holds great potential for the development of rugged, portable, and cost-effective THz systems.

**Acknowledgements** This project was supported by the German minister for education and research within the project "Femtodiode". We thank R. Haferkorn for the numerical implementation of the Drude–Lorentz model.

## References

1. K. Kawase, Y. Ogawa, Y. Watanabe, H. Inoue, Opt. Express **11**, 2549–2554 (2003)
2. H.-B. Liu, Y. Chen, G.J. Bastiaans, X.-C. Zhang, Opt. Express **14**, 415–423 (2006)
3. H. Zhong, J. Xu, X. Xie, T. Yuan, R. Reightler, E. Madaras, X.-C. Zhang, IEEE Sens. J. **5**, 203–208 (2005)
4. S. Wietzke, C. Jansen, F. Rutz, D.M. Mittleman, M. Koch, Polym. Test. **26**, 614–618 (2007)
5. F. Rutz, T. Hasek, M. Koch, H. Richter, U. Ewert, Appl. Phys. Lett. **89**, 221911–221913 (2006)
6. C. Jördens, M. Koch, Opt. Eng. **47**, 037003–037007 (2008)
7. J.A. Zeitler, K. Kogermann, J. Ratanen, T. Rades, P.F. Taday, M. Pepper, J. Aaltonen, C.J. Strachan, Int. J. Pharm. **334**, 78–84 (2007)
8. D.M. Mittleman, R.H. Jacobsen, M.C. Nuss, IEEE J. Sel. Top. Quantum Electron. **2**, 679–692 (1996)
9. S. Hadjiloucas, L.S. Karatzas, J.W. Bowen, IEEE Trans. Microwave Theory Techn. **47**, 142–149 (1999)
10. M. Panzner, W. Köhler, S. Winnerl, M. Helm, F. Rutz, C. Jördens, M. Koch, H. Leitner, U. Klotzbach, E. Beyer, in *9th European Conference on Non-Destructive Testing*, September 2006, Germany (2006)
11. K. Fukunaga, Y. Ogawa, S. Hayashi, I. Hosako, IEICE Electron. Express **4**, 258–263 (2007)
12. S. Verghese, K.A. McIntosh, S. Calawa, W.F. Dinatale, E.K. Duerr, K.A. Molvar, Appl. Phys. Lett. **73**, 3824–3826 (1998)
13. K. Siebert, T. Löffler, H. Quast, M. Thomson, T. Bauer, R. Leonhardt, S. Czasch, H.G. Roskos, Phys. Med. Biol. **47**, 3743–3748 (2002)
14. D. Grischkowsky, S. Keiding, M. van Exter, Ch. Fattinger, J. Opt. Soc. Am. B **7**, 2006–2015 (1990)
15. L. Duvillaret, F. Garet, J.-L. Coutaz, Appl. Opt. **38**, 409–415 (1999)
16. D.J. Derickson, R.J. Helkey, A. Mar, J.R. Karin, J.G. Wasserbauer, J.E. Bowers, IEEE J. Quantum Electron. **28**, 2186–2202 (1992)
17. P.J. Delfyett, C.H. Lee, G.A. Alphonse, J.C. Connolly, Appl. Phys. Lett. **57**, 971–973 (1990)
18. M.G. Thomson, A. Rae, R.L. Sellin, C. Marinelli, R.V. Penty, I.H. White, A.R. Kovsh, S.S. Mikhrin, D.A. Livshits, I.L. Krestnikov, Appl. Phys. Lett. **88**, 133119–133121 (2006)
19. T. Schlauch, M. Li, M.R. Hofmann, A. Klehr, G. Erbert, G. Tränkle, Electron. Lett. **44**, 678–679 (2008)
20. M. Suzuki, M. Tonouchi, Appl. Phys. Lett. **86**, 163504–163506 (2005)

21. N. Chimot, J. Mangeney, L. Joulaud, P. Crozat, H. Bernas, K. Blary, J.F. Lampin, Appl. Phys. Lett. **87**, 193510–193512 (2005)
22. J. Mangeney, N. Chimot, L. Meignien, N. Zerounian, P. Crozat, K. Blary, J.F. Lampin, P. Mounaix, Opt. Express **15**, 8943–8950 (2007)
23. R. Wilk, M. Mikulics, K. Biermann, H. Künzel, I.Z. Kozma, R. Holzwarth, B. Sartorius, M. Mei, M. Koch, in *Conference on Lasers and Electro-Optics* 2007, CThR2 (2007)
24. A. Syouji, S. Saito, K. Sakai, M. Nagai, K. Tanaka, H. Ohtake, T. Bessho, T. Sugiura, T. Hirosumi, M. Yoshida, J. Opt. Soc. Am. B **24**, 2006–2012 (2007)
25. G. Molis, R. Adomavicius, A. Krotkus, K. Bertulis, L. Giniunas, J. Pocius, R. Danielius, Electron. Lett. **43**, 190–191 (2007)
26. D.J.L. Birkin, E.U. Rafailov, W. Sibbet, Appl. Phys. Lett. **80**, 1862–1863 (2002)
27. M. Kolesik, J.V. Moloney, IEEE J. Quantum Electron. **37**, 936–944 (2001)
28. K. Kim, S. Lee, P. Delfyett, Opt. Express **13**, 4600–4606 (2005)
29. B.B. Hu, M.C. Nuss, Opt. Lett. **16**, 1716–1719 (1995)
30. S. Hunsche, D.M. Mittleman, M. Koch, M.C. Nuss, IEICE Trans. Electron. E **81-C**(2), 269–276 (1998)
31. R. Inoue, Y. Ohno, M. Tonouchi, Jpn. J. Appl. Phys. **45**, 7928–7932 (2006)
32. P.U. Jepsen, R.H. Jacobsen, S.R. Keiding, J. Opt. Soc. Am. B **13**, 2424–2436 (1996)
33. D. Grischkowsky, N. Katzenellenbogen, in *Picosecond Electronics and Optoelectronics*, ed. by T. Stollner, J. Shah. OSA Proceedings, Washington, D.C. (1991), pp. 9–14